ISBN: 978-3-95450-262-2 ISSN: 2673-5350 doi: 10.18429/JACoW-IBIC2025-MOPMO32

CHARACTERIZATION OF THE RADIATION ENVIRONMENT IN THE FCC-ee TUNNEL

A. Frasca[1,*], G. Broggi, R. Bruce, B. Humann, A. Lechner, G. Lerner, CERN, Geneva, Switzerland
M. Boscolo, A. Ciarma, INFN, Frascati, Italy
C. Welsch[1], N. Kumar[1], Cockcroft Institute, Sci-Tech Daresbury, Warrington, UK
[1]also at Department of Physics, University of Liverpool, Liverpool, UK

Abstract

The Future Circular e^+e^- Collider (FCC-ee) at CERN will provide collisions at four interaction points along a 91 km long ring, with beam energies ranging from 45.6 GeV (Z pole) to 182.5 GeV ($t\bar{t}$ threshold). The radiation environment along the accelerator varies significantly, with different dominant sources depending on location and operational mode. Accurate characterization of this environment is essential for the design and placement of machine equipment, particularly electronic systems and beam instrumentation. In this study, the Monte Carlo code FLUKA is used to characterize tunnel radiation levels from the main sources, including radiative Bhabha scattering, synchrotron radiation, and beam-gas interactions. The results at the Z pole and $t\bar{t}$ threshold for both the interaction regions and arcs are presented to guide early-stage design considerations and to quantify exposure risks for electronics at potential installation locations.

INTRODUCTION

The first stage of the Future Circular Collider (FCC) at CERN foresees a high-luminosity lepton collider, FCC-ee [1]. The FCC-ee will serve as an electroweak, Higgs and top quark factory by providing e^+e^- collisions at four interaction points (IPs) along a 91 km long ring. It will cover beam energies from 45.6 GeV (Z pole) to 182.5 GeV ($t\bar{t}$ threshold). The power radiated as synchrotron radiation (SR) is by design limited to 50 MW/beam across all the operational modes by adjusting the beam current according to the energy. At the Z pole, the beam current reaches 1294 mA with a luminosity per IP of $145 \times 10^{34}\,\mathrm{cm^{-2}\,s^{-1}}$, while at the $t\bar{t}$ threshold the current is reduced to 5.1 mA, with a corresponding luminosity of $1.41 \times 10^{34}\,\mathrm{cm^{-2}\,s^{-1}}$.

Characterizing the tunnel radiation environment is essential for the safe operation of machine equipment and electronics and directly influences the design of beam instrumentation systems, such as beam loss monitors (BLMs) and beam position monitors (BPMs). This task is particularly challenging at FCC-ee, where variations in beam parameters across operational modes lead to significant shifts in the dominant radiation sources and, consequently, in the environment throughout the accelerator.

In circular lepton machines, SR is a major source of radiation, as the energy loss per turn scales with $\frac{E^4}{m_e^4 \rho}$, where E is the beam energy, m_e the electron mass, and ρ the bending radius. Although the SR power loss is kept constant by design for all FCC-ee operating points, the tunnel radiation levels strongly depend on the photon energy spectrum, defined by the critical energy $E_c \propto \frac{E^3}{\rho}$. This value is 0.02 MeV at the Z pole, where photons have a short attenuation length and are mostly absorbed in the vacuum chamber, making tunnel leakage negligible. At the $t\bar{t}$ threshold, the harder photon spectrum ($E_c = 1.3$ MeV) produces radiation showers beyond the chamber, making SR a dominant concern for the tunnel environment. On the other hand, the Z pole mode is more affected by beam loss mechanisms that scale with beam intensity, such as beam-gas (BG) interactions, and by collision-induced losses driven by luminosity. As a result, while the most severe radiation environment in the FCC-ee arcs occurs at the $t\bar{t}$ mode due to SR, the interaction regions (IRs) around the IPs present a critical scenario even at the Z mode, with contributions from radiative Bhabha (RB) scattering, beamstrahlung (BS) and secondary particles from collimators upstream of the experiment.

In this work, the Monte Carlo code FLUKA [2–4] is used to simulate radiation showers from the main sources and to estimate dose levels in FCC-ee tunnel. The aim is to provide an early characterization of the expected radiation environment and support the development of design strategies. The study does not quantify the beam loss sources for which BLMs must be designed, but rather highlights the radiation conditions in which different systems will have to operate. Results are presented for a representative arc section at the $t\bar{t}$ mode, and for a generic IR at both Z and $t\bar{t}$ modes, allowing comparison across operational scenarios.

SIMULATION SETUP

Geometries representative of a FCC-ee arc section and IR for V24.4 of the Global Hybrid Correction lattice [5–7] were implemented in FLUKA, including the main beamline elements and tunnel infrastructure relevant to radiation transport. Magnet and tunnel models are based on Refs. [1, 8]. A 2 mm-thick copper beam pipe with a radius of 30 mm and horizontal winglets is assumed. The horizontal winglets of the dipole vacuum chambers embed 37 cm long discrete photon stoppers made of a copper alloy (CuCrZr), designed to intercept SR photons [9–12]. The arc model features a $t\bar{t}$ FODO cell, with a length of about 52 m. Previous studies have highlighted the need for additional shielding around the photon stoppers, as well as the effectiveness of preliminary shielding concepts [13, 14]. The present arc shielding layout builds upon the configuration presented in [15], now featuring a bulkier photon stopper and a simplified shield-

* alessandro.frasca@cern.ch

ISBN: 978-3-95450-262-2 ISSN: 2673-5350 doi: 10.18429/JACoW-IBIC2025-MOPMO32

ing geometry without internal parts [16]. The IR model follows the geometry presented in Ref. [17], covering a longitudinal range of 725 m from one side of the experiment and including both incoming and outgoing beamlines. The incoming beamline hosts SR masks, SR collimators (TCRs), and two tertiary collimators, one vertical (TCTV) located at s = 456 m and one horizontal (TCTH) at 706 m upstream of the IP. The model has been updated to incorporate the same discrete SR absorbers implemented in the arcs, though no dedicated radiation shielding has been studied or included at this stage.

While SR photons can be directly generated in FLUKA during particle transport in vacuum within magnetic fields, the other radiation sources require dedicated treatments. As detailed in Ref. [17], RB particles are sampled from distributions generated with the external codes BBBREM [18] and GUINEA-PIG++ [19]. The contribution from BS, which is extracted toward a dedicated dump, is not considered here. It is assumed to be fully contained by a shielding system specifically designed to meet radiation protection criteria, not addressed in this work. For BG interactions, only the contribution from the resulting losses on the collimators is taken into account. Specifically, BG Coulomb scattering and bremsstrahlung processes were simulated in multi-turn tracking simulations [20] performed with Xsuite [21], considering a pessimistic gas pressure profile corresponding to only 1 h of beam conditioning. Collimator hit data were recorded and used as input to sample losses in the IR FLUKA model. Losses in the collimators at the IR furthest from the collimation insertion were selected, as this represents the most critical case.

FCC-ee ARCS

In the arcs, SR is the dominant source of tunnel radiation at the $t\bar{t}$ operating point. At the Z mode the environment is expected to be dominated by beam losses due to BG scattering, which are not yet fully characterized. Accordingly, the results presented here focus exclusively on the SR-induced effects at $t\bar{t}$. Figure 1 shows the top-view distribution of total ionising dose (TID) at beam level, accumulated over one year assuming 185 days of operation at 75 % efficiency and design beam currents. At the locations of the photon stoppers, the TID exceeds 100 MGy yr^{-1} inside the dipole magnets. The additional lead shielding effectively reduces radiation

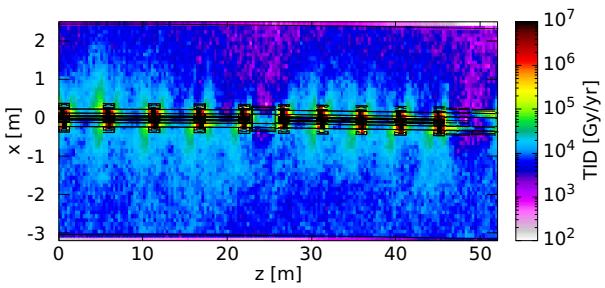

Figure 1: Top view (average over ±50 cm in y) of annual SR-induced TID in an arc FODO cell at $t\bar{t}$ mode.

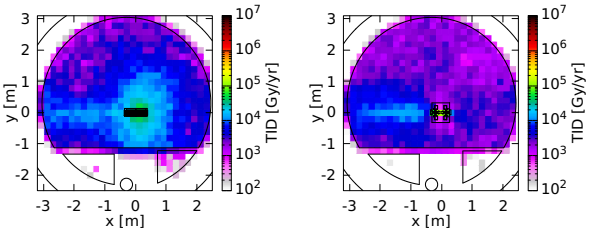

Figure 2: Annual SR-induced TID in the FCC-ee arc at the $t\bar{t}$ mode: at photon stopper (left) and at quadrupole (right).

leakage, containing the TID to around 10 kGy yr^{-1} outside the dipoles, with regions up to 100 kGy yr^{-1} close to shielding locations. Nevertheless, instrumentation located near the vacuum chamber, along with their attached cables, must withstand MGy-level TIDs and therefore requires radiation-hard design. Radiation levels around the quadrupoles are less critical, remaining below 10 kGy yr^{-1}.

Cross-sectional views of the TID distribution (Fig. 2) indicate that, at the upper cable tray level (at the tunnel wall above 2 m from floor level), the annual TID reaches approximately 10 kGy yr^{-1}. Considering 5 yr of $t\bar{t}$ operation, plus smaller contributions from the other modes [15], the cumulative dose remains below 100 kGy for most cables, making the use of general-purpose cabling compatible with CERN current qualification criteria. The harsh radiation environment would require the use of costly rad-hard components for electronics that has to be installed in the tunnel. Radiation-tolerant devices based on commercial-off-the-shelf (COTS) components can be developed, but their deployment would be restricted to areas where the cumulative TID does not exceed 0.5–1 kGy. To enable the use of such systems, the option of housing electronics racks in dedicated bunkers is being explored [15]. The current design foresees concrete bunkers (20 cm thick walls) located below the dipoles, effectively stopping SR-induced electromagnetic showers. However, neutrons from photonuclear reactions can still penetrate the walls and dominate the radiation effects inside the bunker, also exposing the electronics to single event effects. To mitigate this, the inner bunker walls are lined with borated polyethylene sheets, which help moderate and capture neutrons. Table 1 shows key radiation metrics for cumulative (dose D, 1 MeV-neutron-equivalent fluence in Silicon $\Phi_{eq}^{1\,\mathrm{MeV}}$) and single-event (high-energy hadron-equivalent fluence Φ_{eq}^{HEH} and thermal neutron-equivalent fluence Φ_{eq}^{THN}) effects, indicating that conditions inside the proposed bunker are comparable or better than those expected in the HL-LHC arcs (below magnets). Since the neutron spectrum at FCC-ee

Table 1: Comparison Between Radiation Environment in the FCC-ee Bunker and the HL-LHC Arcs

	FCC-ee $t\bar{t}$	HL-LHC
D	<10 Gy yr^{-1}	1.4 Gy yr^{-1}
$\Phi_{eq}^{1\,\mathrm{MeV}}$	7×10^9 cm^{-2} yr^{-1}	1.6×10^{10} cm^{-2} yr^{-1}
Φ_{eq}^{HEH}	1×10^7 cm^{-2} yr^{-1}	2.4×10^9 cm^{-2} yr^{-1}
Φ_{eq}^{THN}	4×10^9 cm^{-2} yr^{-1}	1.2×10^{10} cm^{-2} yr^{-1}

ISBN: 978-3-95450-262-2 ISSN: 2673-5350 doi: 10.18429/JACoW-IBIC2025-MOPMO32

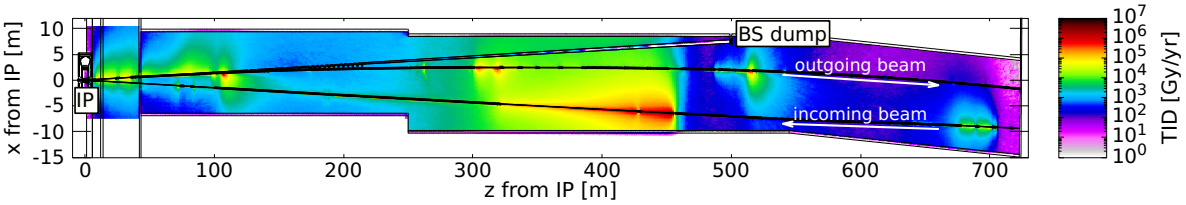

(a) Top view (average over ±20 cm in y) of annual TID from RB and BG losses on collimators at Z pole as simulated with FLUKA.

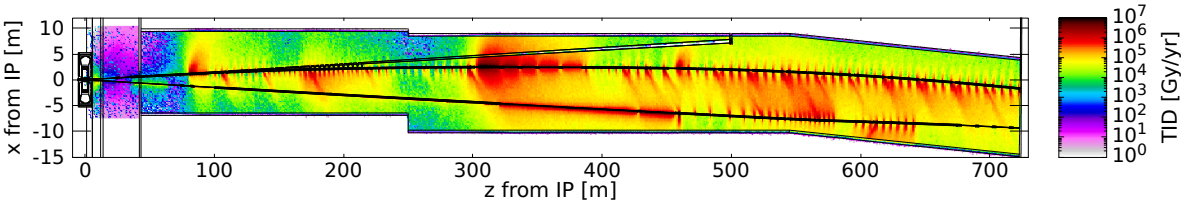

(b) Top view (average over ±20 cm in y) of annual TID from SR and RB at $t\bar{t}$ as simulated with FLUKA.

Figure 3: Comparison of annual TID distributions in a symmetric half of the IR at Z (a) and $t\bar{t}$ (b) operational modes.

differs from that in LHC, shielding and electronics response will require dedicated studies beyond the scope of this paper. Nevertheless, with proper design, COTS-based electronics could be deployed in such protected environments.

FCC-ee INTERACTION REGIONS

In the IRs, the radiation environment is shaped by multiple sources depending on the FCC-ee operating point. For all modes, the SR power in this region is about 310 kW along the outgoing beamline and 90 kW along the incoming one. At the Z pole, the SR has a E_c of only a few tens of keV, therefore the radiation environment is dominated by off-momentum products from RB events at the IP, as well as by showers from the upstream collimators. The top-view distribution of annual TID for the Z pole (Fig. 3a) includes contributions from RB e^+ and beam losses on TCRs, TCTV and TCTH due to BG Coulomb scattering and bremsstrahlung interactions. Local BG losses within the simulated geometry are neglected here, as preliminary checks have shown that local BG bremsstrahlung produces negligible dose hotspots below 0.1 kGy yr^{-1} even under pessimistic conditions. Radiative Bhabha losses create hotspots of 10–100 kGy yr^{-1} along the outgoing beamline at sections with reduced material budget, such as drifts or magnets accommodating the BS extraction line [8]. These losses dominate within 150 m from the IP and in isolated spots near 300 m and 515 m from the IP. Such localized hotspots depend on the specific RB loss distribution, which is determined by the beam optics, and scale proportionally with luminosity. Radiation levels between 200 m and 450 m are entirely dominated by BG Coulomb losses on the TCTV, reaching up to fractions of a MGy yr^{-1} along the drift downstream of the collimator. Between 600 m and 700 m from the IP, BG Coulomb and bremsstrahlung losses on the TCTH contribute roughly equally to a hotspot of less than 10 kGy yr^{-1}. The contribution from BG collimation losses is currently less reliable, as it depends on factors with significant uncertainties, such as optics, collimation design, and vacuum pressure profiles. However, the estimate is conservative, since it assumes a pressure after only 1 h of beam conditioning, whereas over a full year of operation the more conditioned vacuum should significantly reduce BG losses.

In contrast, at the $t\bar{t}$ operating point, SR has a E_c of about 1 MeV and dominates over RB and BG interactions, due to the lower beam current and luminosity. The $t\bar{t}$ dose map (Fig. 3b), including only RB and SR, shows SR producing widespread dose levels along the beamlines, overshadowing RB contributions. Hotspots of 0.1–1 MGy yr^{-1} occur at photon stopper locations and drifts not shadowed by them.

Overall, radiation levels in the IRs exceed the tolerance of standard machine equipment at all operating points. This calls for dedicated shielding, including absorbers for RB products, shower absorbers downstream of TCTs, dipole shielding as in the arcs, and protection of exposed drifts. Notably, radiation showers from non-SR sources start from GeV-level particles, whereas SR-induced showers at $t\bar{t}$ arise from MeV-scale photons, influencing shielding design. Once these measures are in place, potential in-tunnel electronics locations and dedicated protection solutions should be studied to enable the safe deployment of radiation-tolerant systems.

CONCLUSION

This work presents an overview of FCC-ee tunnel radiation levels, focusing on the arcs and the IRs. FLUKA simulations show that in the arcs, at the $t\bar{t}$ operational mode, the SR-dominated radiation environment can be mitigated through a combination of photon stoppers and shielding. This likely allows the deployment of general-purpose cables on trays routing to protected alcoves. Despite the shielding, instruments on the beamline, such as BPMs, and their cable connectors must withstand high radiation levels and be qualified for MGy doses. Dedicated electronics bunkers may enable the use of cost-effective COTS-based systems for in-tunnel electronics. In the IRs, high radiation levels arise not only from SR at $t\bar{t}$ but also from RB products and collimator showers at the Z pole. Mitigation strategies analogous to those in the arcs must be developed and adapted to the specific requirements of each operating mode.

ISBN: 978-3-95450-262-2 ISSN: 2673-5350 doi: 10.18429/JACoW-IBIC2025-MOPMO32

REFERENCES

[1] M. Benedikt *et al.*, "FCC-ee: The Lepton Collider: Future Circular Collider Conceptual Design Report Volume 2", CERN, Geneva, Switzerland, Rep. CERN-ACC-2018-0057, Dec. 2018. doi:10.1140/epjst/e2019-900045-4

[2] FLUKA website, https://fluka.cern/.

[3] G. Battistoni *et al.*, "Overview of the FLUKA code", *Ann. Nucl. Energy*, vol. 82, pp. 10–18, 2015. doi:10.1016/j.anucene.2014.11.007

[4] C. Ahdida *et al.*, "New Capabilities of the FLUKA Multi-Purpose Code", *Front. Phys.*, vol. 9, pp. 1–14, 2022. doi:10.3389/fphy.2021.788253

[5] K. Oide *et al.*, "Design of beam optics for the future circular collider e^+e^- collider rings", *Phys. Rev. Accel. Beams*, vol. 19, p. 111 005, 2016. doi:10.1103/PhysRevAccelBeams.19.111005

[6] K. Oide, "Optics with finite chromaticities", presented at 193rd FCC-ee Accelerator Design Meeting, CERN, Meyrin, Switzerland, Oct. 2024.

[7] CERN optics repository, https://acc-models.web.cern.ch/acc-models/fcc/.

[8] C. J. Eriksson, "Magnet design for beamstrahlung photons extraction line", presented at FCC week 2023, London, Jun. 2023.

[9] R. Kersevan, "Vacuum System of the FCC-ee", in *Proc. eeFACT'22*, Frascati, Italy, Sep. 2022, pp. 244–246. doi:10.18429/JACoW-eeFACT2022-THXAS0104

[10] R. Kersevan and C. Garion, "Conceptual Design of the Vacuum System for the Future Circular Collider FCC-ee Main Rings", in *Proc. IPAC'21*, Campinas, Brazil, May 2021, pp. 2438–2440. doi:10.18429/JACoW-IPAC2021-TUPAB392

[11] R. Kersevan, "The FCC-ee vacuum system, from conceptual to prototyping", *EPJ Tech. Instr.*, vol. 9, no. 12, pp. 1–9, 2022. doi:10.1140/epjti/s40485-022-00087-w

[12] M. Morrone, C. Garion, P. Chiggiato, R. Kersevan, and S. Rorison, "Preliminary design of the FCC-ee vacuum chamber absorbers", in *Proc. IPAC'23*, Venice, Italy, May 2023, pp. 382–385. doi:10.18429/JACoW-IPAC2023-MOPA141

[13] B. Humann, F. Cerutti, and R. Kersevan, "Synchrotron Radiation Impact on the FCC-ee Arcs", in *Proc. IPAC'22*, Bangkok, Thailand, Jun. 2022, pp. 1675–1678. doi:10.18429/JACoW-IPAC2022-WEPOST002

[14] B. Humann *et al.*, "Challenges and mitigation measures for synchrotron radiation on the FCC-ee arcs", in *Proc. IPAC'24*, Nashville, TN, USA, May 2024, pp. 292–295. doi:10.18429/JACoW-IPAC2024-MOPG04

[15] A. Lechner *et al.*, "FCC-ee radiation environment and shielding", in *Proc. IPAC'25*, Taipei, Taiwan, Jun. 2025, pp. 482–485. doi:10.18429/JACoW-IPAC25-MOPM068

[16] B. Humann, "Radiation environment in the FCC-ee arcs", presented at FCC week 2025, Vienna, May 2025.

[17] A. Frasca *et al.*, "Radiation load from radiative bhabha scattering in the FCC-ee experimental insertions", in *Proc. IPAC'25*, Taipei, Taiwan, Jun. 2025, pp. 478–481. doi:10.18429/JACoW-IPAC25-MOPM067

[18] R. Kleiss and H. Burkhardt, "BBBREM — Monte Carlo simulation of radiative Bhabha scattering in the very forward direction", *Comput. Phys. Commun.*, vol. 81, pp. 372–380, 1994. doi:10.1016/0010-4655(94)90085-X

[19] C. Rimbault *et al.*, "GUINEA-PIG++ : An Upgraded Version of the Linear Collider Beam-Beam Interaction Simulation Code GUINEA-PIG", in *Proc. PAC'07*, Albuquerque, NM, USA, Jun. 2007, pp. 2728–2730. doi:10.1016/0010-4655(94)90085-X

[20] G. Broggi *et al.*, "Beam losses due to beam-residual gas interactions in the FCC-ee", in *Proc. IPAC'25*, Taipei, Taiwan, Jun. 2025, pp. 390–393. doi:10.18429/JACoW-IPAC25-MOPM036

[21] G. Iadarola *et al.*, "Xsuite: An Integrated Beam Physics Simulation Framework", in *Proc. HB'23*, Geneva, Switzerland, Mar. 2024, pp. 73–80. doi:10.18429/JACoW-HB2023-TUA2I1